

Probing vacuum birefringence under a high-intensity laser field with gamma-ray polarimetry at the GeV scale

Yoshihide Nakamiya,¹ Kensuke Homma,^{2,3,*} Toseo Moritaka,⁴ and Keita Seto⁵

¹*Advanced Research Center for Beam Science, Institute for Chemical Research,
Kyoto University, Gokasho, Uji, Kyoto 611-0011, Japan*

²*Graduate School of Science, Hiroshima University,
Kagamiyama, Higashi-Hiroshima, Hiroshima 739-8526, Japan*

³*International Center for Zetta-Exawatt Science and Technology,
Ecole Polytechnique, Route de Saclay, F-91128 Palaiseau Cedex, France*

⁴*National Central University, Taiwan*

⁵*Extreme Light Infrastructure - Nuclear Physics (ELI-NP)/Horia Hulubei
National Institute for R&D in Physics and Nuclear Engineering (IFIN-HH),
30 Reactorului St., Bucharest-Magurele, jud. Ilfov, P.O.B. MG-6, RO-077125, Romania*
(Dated: December 1, 2015)

Probing vacuum structures deformed by high intense fields is of great interest in general. In the context of quantum electrodynamics (QED), the vacuum exposed by a linearly polarized high-intensity laser field is expected to show birefringence. We consider the combination of a 10 PW laser system to pump the vacuum and 1 GeV gamma-rays to probe the birefringent effect. The vacuum birefringence can be measured via the polarization flip of the probe gamma-rays. We discuss the design of the gamma-ray polarimeter and then evaluate the measurability of the reduction of the degree of linear polarization due to the appearance of birefringence. We found that the measurement is indeed feasible given a realistic set of laser parameters and achievable pulse statistics.

PACS numbers: 12.20.-m, 12.20.Fv, 41.75.Jv, 25.75.Cj

The quantum nature of the vacuum in various extreme conditions is an intriguing subject to explore. The vacuum structure can be deformed by the existence of external fields, such as gravitational fields [1] and electromagnetic fields [2]. It can also be modified by special boundary conditions via Casimir effects [3]. Common observables in these vacuum states are the dispersion relation for probe radiation and polarization dependence [4]. One interesting question is how much these properties differ between the present and the early Universe when field densities were extremely high for certain boundary conditions [5]. These properties are governed by the virtual quanta contained in the vacuum immersed in these intense fields, and the dominant virtual quanta differ depending on the dynamics. Therefore, the energy scale of the probe radiation is an important factor as well as the external field strength.

Understanding the interactions of probe radiation with external fields requires non-trivial field theoretical treatments in the non-perturbative regime, where summing up all-order Feynman diagrams is necessary. Among various types of intense fields, the theoretical predictions in the simplest QED case naturally become the first candidates to be thoroughly tested by laboratory experiments. Although there are a number of theoretical calculations based on different schemes applied to constant and time-varying field configurations [6–8], to date there has been no direct experimental verification in pristine initial and final state conditions. The rapid development of high-intensity laser facilities, such as the Extreme Light Infrastructure (ELI) [9], leads us to con-

sider testing the propagation properties in focused pump laser fields. Once the calculation schemes have been tested in the context of QED, non-perturbative predictions can be reliably applied to more complicated intense fields: for instance, those in strongly magnetized compact stars, such as magnetars [10], and the early-stage of quark-gluon plasmas accompanying thermal photons in relativistic heavy-ion collisions [11], where interference between intense QED and intense quantum chromodynamic fields is expected [12, 13].

The optical phase retardation, Γ , between mutually orthogonal components of linearly polarized probe radiation is given by $\Gamma = 2\pi\Delta n L \lambda^{-1}$, where λ is the wave length of the probe radiation, Δn is the relative refractive index change between the two orthogonal components induced by the pump field and L is the length of the birefringent region.

Several experiments have attempted to measure the magnetic birefringence of the vacuum [14–16]. For example, the PVLAS experiment [14] can realize $\Delta n = 4 \times 10^{-23}$ and $\Gamma = 5 \times 10^{-11}$. That experiment utilizes the advantage of a static magnetic field to increase the phase shift using the long path length of the interaction region, which compensates for the smallness of Δn . These measurements, however, require careful control of the vacuum pressure, because the probe radiation interacts with residual atoms in the interaction region in the vacuum chamber.

In contrast to this approach utilizing a long L , we may consider combining a high-intensity pump laser and a high-energy probe to simultaneously increase Δn and

phase retardation with a much shorter λ . Multi-petawatt class lasers have the capability of enhancing the relative refractive index change to $\Delta n \sim 10^{-10}$ [17]. The use of X-ray probes was proposed by Marx et al. [18].

In this letter we consider extending the probe energy up to the GeV regime by exploiting intense lasers to obtain a linearly polarized gamma-ray source in order to realize $\Gamma \sim 1$. Widening the probe energy range will allow complete measurement of the dispersion relation and enable accurate comparisons with the QED predictions.

The phase shift may be interpreted as being a consequence of polarization flips of gamma-rays. The degree of polarization of gamma-rays is defined as

$$P_l = \frac{N_{\parallel} - N_{\perp}}{N_{\parallel} + N_{\perp}}, \quad (1)$$

where N_{\perp} and N_{\parallel} are, respectively, the numbers of gamma-rays with linear polarization states perpendicular and parallel to the direction of the linear polarization of the pump laser. The polarization-flip phenomenon in an intense pump field has been discussed and quantified by Dinu et al. [19]. Suppose gamma-rays with energy, ω , collide head-on with a focused laser having a Gaussian profile, as illustrated in Fig. 1, the flipping probability of probe gamma-rays is given by

$$P(\omega, \psi) = \left(\frac{\alpha}{15} \frac{1}{E_s^2} \frac{\epsilon \omega}{\pi^2 w_0^2} \right)^2 e^{-\frac{4\psi^2}{\psi_0^2}} \quad (2)$$

with $\psi_0 = \tan^{-1} \frac{w_0}{l},$

where α is the fine structure constant, E_s is the Schwinger critical electric field, w_0 is the waist size of the focused laser, ϵ is the energy of the pump laser, ψ is the emission angle of gamma-rays with respect to the head-on direction and l is the distance between the interaction point and the gamma-ray production point. The effect of the angular dispersion of gamma-rays or misalignment with respect to the head-on collisions is expressed as the exponential reduction of the flipping probability. The experimental observable in the vacuum pump-probe method with a gamma-ray probe is the reduction of the degree of linear polarization from P_l to $[1 - 2P(\omega, \psi)] P_l$.

We now consider the concrete design of the experiment illustrated in Fig. 1 for the measurement of the polarization-flip effect caused by laser-induced birefringence. We first require that the probe gamma-ray energy is not too high in order to avoid tunneling electron-positron pair production in the intense pump field. We assume 1 GeV probe gamma-rays in the following discussion. We simultaneously need a high degree of linear polarization for the probe gamma-ray. Given a 10 PW-class laser, which is available at the ELI project with a typical wavelength of 800 nm, we can produce linearly polarized gamma-rays by Compton scattering between the linearly polarized laser pulse and unpolarized electron bunches. We will assume that 5 GeV

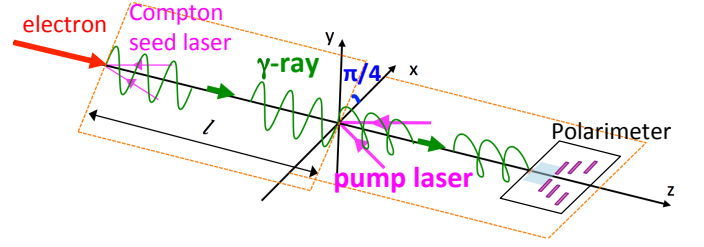


FIG. 1: Conceptual experimental setup to investigate vacuum birefringence via the reduction of the degree of linear polarization of probe gamma-rays.

electrons collide with the laser pulses head-on. The assumed electron energy is reasonable given the successful production of quasi-monoenergetic electrons at 4.2 GeV [20] using the laser-plasma acceleration technique [21, 22]. The gamma-ray yields are estimated by using published cross sections [23, 24] for nonlinear Compton scattering with laser power $6.66 \times 10^{10} \text{ W}$ and intensity $8.28 \times 10^{17} \text{ W/cm}^2$, resulting in a nonlinearity parameter $\eta \equiv e\sqrt{-\langle A_{\mu} A^{\mu} \rangle}/mc^2 = 0.62$, where A_{μ} is the four-vector potential of the laser pulse. Gamma-rays at GeV energies are produced by the multi-photon absorption process in nonlinear Compton scattering and emitted within a cone angle of $1/\gamma_e$ rad, where γ_e is the Lorentz factor of the electrons. We consider gamma-rays with an energy of 1.01 - 1.02 GeV and emission angle less than or equal to $1/10\gamma_e = 1.022 \times 10^{-5}$ rad. This energy range corresponds to the case when the number of absorbed laser photons reaches 3. The limitation of the emission angle is actually necessary to select highly polarized gamma-rays. With a time integrated luminosity over the laser pulse duration of $4.0 \times 10^{23} \mu\text{m}^{-2}$ and assuming 10^9 electrons, the integrated numbers of gamma-rays over that angular range are evaluated for both the same polarization as the incident Compton seed laser pulse and the orthogonal polarization. The degree of linear polarization is estimated to be $P_l = 0.97$ for the above conditions.

We now consider the case where the generated polarized gamma-rays penetrate through the focal region of the pump laser after traveling a distance l . Assuming a conservative waist size for the focal spot of $w_0 = 2.4 \mu\text{m}$, a wavelength of 800 nm, a pulse energy of 200 J and an intensity of $3.7 \times 10^{22} \text{ W/cm}^2$, the degree of linear polarization of the incident gamma-rays is expected to change from $\langle P_l \rangle = 0.97$ to $\langle [1 - 2P(\omega, \psi)] P_l \rangle = 0.53$ after passing through the laser-induced birefringent vacuum, where $\langle \dots \rangle$ represents the weighted mean of the degree of the polarization over the angular range from $\psi = 0$ to $\psi = 1/10\gamma_e$ and the flipping probability, $P(\omega, \psi)$, has been calculated with the given laser parameters and $l = 10 \text{ cm}$.

Figure 2 (a) shows the incident gamma-ray spectra as

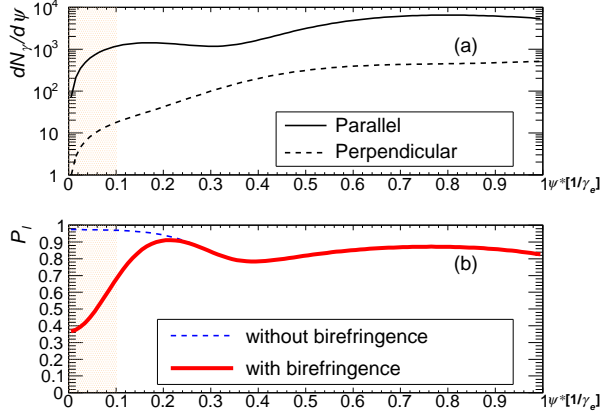


FIG. 2: (a) The incident gamma-ray yield as a function of the emission angle for each polarization state. (b) The degree of linear polarization of gamma-rays. The polarization-flip effect due to the laser-induced birefringence depends on the emission angle.

a function of the emission angle with respect to the direction of the incident electron. The horizontal axis ψ^* in Fig. 2 (a) is the deduced emission angle, which is normalized to the inverse of the Lorentz factor for 5 GeV electrons. The components parallel and perpendicular to the polarization direction of the Compton seed laser are depicted by solid and dotted lines, respectively. The polarization-flip effect appears as a reduction of the degree of linear polarization, as shown in Fig.2 (b). A large polarization-flip effect becomes visible in the forward direction, especially for $\psi < 1/10\gamma_e$. We note that the reference polarization plane must be parallel to the direction of the polarization of the Compton seed laser and the pump laser must be aligned with a relative rotation angle of $\pi/4$ from that reference plane. This configuration produces equal amplitudes for mutually orthogonal electromagnetic field components of probe photons and, hence, maximizes the visibility of the polarization-flip effect.

The polarization of gamma-rays with energies above 100 MeV can be reconstructed by the kinematical relations for the conversion process from a gamma-ray into an electron-positron pair [25, 26]. The degree of linear polarization of the incident gamma-rays is characterized by the anisotropic angular distribution of the reaction plane containing the electron-positron pair with respect to the polarization plane of the incident gamma-rays [27–33]. The angular dependence of the e^-e^+ pair emission caused by gamma-rays with linear polarization P_l is given by

$$\frac{dN_{ee}^{pol}}{d\phi} = N_{ee} (1 + P_l A \cos 2\phi), \quad (3)$$

where N_{ee} is the number of e^-e^+ pairs in the unpolarized case and ϕ is the angle of the e^-e^+ reaction plane with

respect to the polarization plane of the incident gamma-rays. The analyzing power, A , refers to the reduction of anisotropy caused by experimental biases.

There are two key issues in the design of the gamma-ray polarimeter. The first is how to deal with a large number of gamma-rays confined within a cone angle of $1/10\gamma_e$. In our estimation, $\sim 5 \times 10^3$ gamma-rays at 1 GeV are expected to enter into a detector at a time. For this purpose, the gamma-ray converter must be carefully chosen in order to adjust the number of e^-e^+ pairs depending on the handling capability of the polarimeter. To accurately spot the $1/10\gamma_e$ range, we need to locate the converter far from the interaction point. If the converter is located at 10 m, the angular range corresponds to a resolution of $10 \mu\text{m}$. Therefore, a pixel size below $10 \mu\text{m} \times 10 \mu\text{m}$ is not necessary as long as we assume a fixed incident point on the converter in the track reconstruction algorithm. Thus the position resolution is required to be around $10 \mu\text{m}$ at most. The second issue is how to accurately reconstruct a reaction plane based on the momentum vectors of an e^-e^+ pair produced at the conversion point, which has the greatest effect on the analyzing power in the end. The opening angle of a pair at the conversion point is the key information needed to correctly reconstruct the anisotropy in Eq.(3). The original angle is, however, smeared by multiple Coulomb scatterings during passage through the conversion material. In addition, multiple Coulomb scatterings inside each pixel sensor also give rise to a displacement of the measured hits from the ideal trajectory of a charged particle. This displacement degrades the track finding and reconstructing capabilities and reduces the analyzing power. Thus, the thickness of the detector materials must be controlled to keep the analyzing power at an acceptable level.

The minimum elements of the detector design are illustrated in Fig.3. The detection system simultaneously performs spectroscopy and polarimetry for a multiple gamma-ray injection. It is composed of a converter at the front, a static magnetic field, and three-layers of pixel sensors. The converter is chosen to suppress the smearing effect due to multiple Coulomb scatterings but to keep the pair creation efficiency reasonably high. These two requirements are in a trade-off relation as a function of the thickness and the atomic number of the conversion material. We assume a gold foil with a thickness of $2 \mu\text{m}$ resulting in a conversion efficiency of 10^{-4} in order to expect a single pair per shot if 10^4 gamma-rays are assumed to be incident. A sub-tesla field strength for the static magnetic field provided just behind the converter is enough to measure the sub-GeV momenta of the charge-separated electrons and positrons. To provide this field, a permanent-magnet-based dipole would be preferable from the point of view of the compactness and homogeneity of the field. The three-layered position sensors made of silicon pixels are located downstream of the magnet system. A pixel size of $20 \mu\text{m}$ is reasonable

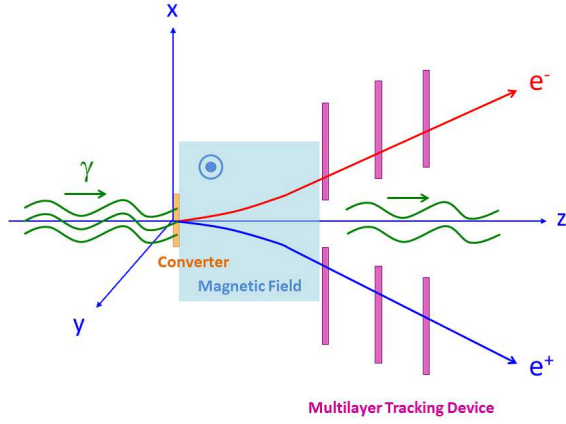


FIG. 3: Detector configuration for gamma-ray polarimetry via gamma-converted e^-e^+ pairs.

to separate electrons and positrons confined in a narrow angular region. The thickness of the pixel sensor is also important to accurately reconstruct true charged tracks from multiple Coulomb scatterings. A reasonable thickness would be below $50 \mu\text{m}$.

The feasibility of performing the gamma-ray polarimetry with the detector configuration illustrated in Fig.3 was evaluated using the Geant4 simulation toolkit[34, 35]. A gamma-ray energy can be reconstructed from the measured momenta of an e^-e^+ pair with an energy resolution of 3.8% at $\omega = 1 \text{ GeV}$. This energy resolution is sufficient to select a narrow enough energy range to guarantee the degree of linear polarization of incident 1.01-1.02 GeV gamma-rays based on the offline selection of pairs. The degree of birefringence can be observed via the reduction of the degree of linear polarization from $\langle P_l \rangle = 0.97$ to $\langle [1 - 2P(\omega, \psi)] P_l \rangle = 0.53$ as shown in Fig.4, which depicts the expected angular distributions of the pair reaction planes with respect to the reference plane. We assume the creation of a single e^-e^+ pair per shot via the conversion process with a total pair statistics of 10^4 in this simulation. The open blue points show the angular distribution of the pair plane in the non-flipping case. The amplitude, $P_l A$, can be determined within a statistical fluctuation of 10% which is equivalent to 3σ . Therefore, this polarimeter design has the capability of excluding the 97% polarization case with respect to the 53% polarization at a significance level of more than 5σ . The flipping case with 53% polarization is shown using filled red points.

In conclusion, we have considered combining a 10 PW laser system with 1 GeV linearly polarized probe gamma-rays to enhance the sensitivity of the measurement of the vacuum birefringence. The vacuum birefringence can be observed by measuring the polarization-flip effect with respect to the linearly polarized probe gamma-rays by utilizing the conversion process of a gamma-ray into an

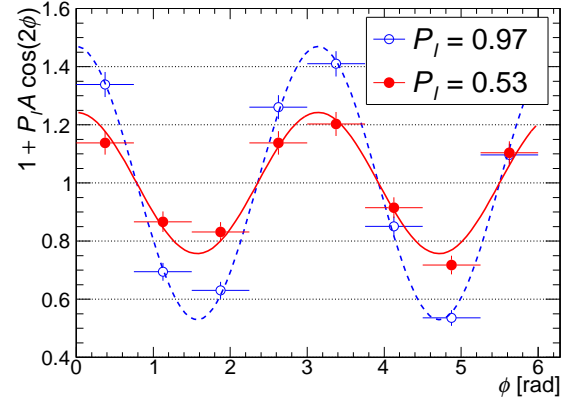


FIG. 4: The angular distributions of the e^-e^+ pair planes with respect the reference plane.

e^-e^+ pair after passing through 10 PW focused pump laser pulses if 10^4 pairs are available. This result is based on a realistic set of laser parameters and potentially realizable statistics for a 10 PW system.

Given the firm theoretical and experimental footing in the simplest QED case, the proposed approach would open up a new arena of fundamental physics to explore more dynamical and complicated vacuum states realized in laboratories, astrophysical objects and possibly the early Universe.

We are grateful to A. Ilderton for detailed discussions and helpful suggestions to quantify the flipping probabilities of gamma-rays. We also thank S. Sakabe, M. Hashida, and S. Inoue for providing many insights into this subject. K. Homma acknowledges for the support by the Collaborative Research Program of the Institute for Chemical Research, Kyoto University (grants No. 2015-93). K. Seto acknowledges the support of the Extreme Light Infrastructure - Nuclear Physics (ELI-NP) - Phase I project, which is co-financed by the Romanian Government and the European Union through the European Regional Development Fund.

-
- * Corresponding author: homma@hepl.hiroshima-u.ac.jp
- [1] I. T. Drummond, S. J. Hathrell, Phys. Rev. D **22**, 343 (1980).
 - [2] J.S. Toll, *The Dispersion Relation for Light and its Application to Problems Involving Electron Pairs*, Ph.D thesis, Princeton University, 1952 (unpublished)
 - [3] K. Scharnhorst, Phys. Lett. B **236**, 354 (1990).
 - [4] G. M. Shore, Nucl. Phys. B **778**, 219 (2007)
 - [5] Joao Magueijo, Rept. Prog. Phys. **66**, 2025 (2003); S. Alexander and J. Magueijo, hep-th/0104093.
 - [6] W. Dittrich and H. Gies, *Probing the Quantum Vacuum*, Springer, Berlin (2007).
 - [7] A. Di Piazza, C. Müller, K. Z. Hatsagortsyan, and C. H.

- Keitel, Rev. Mod. Phys. **84**, 1177 (2012).
- [8] V. Dinu, T. Heinzl, A. Ilderton, M. Marklund and G. Torgrimsson, Phys. Rev. D **89**, 125003 (2014).
- [9] <http://www.eli-laser.eu/>
- [10] C. Thompson and R. C. Duncan, Mon. Not. Roy. Astron. Soc. **275** (1995) 255; *ibid.* Astrophys. J. **473** (1996) 322.
- [11] A. Adare *et al.*, Phys. Rev. Lett. **104**, 132301 (2010).
- [12] D. E. Kharzeev, L. D. McLerran, and H. J. Warringa, Nucl. Phys. A **803**, 227-253 (2008).
- [13] Sho Ozaki, Takashi Arai, Koichi Hattori, and Kazunori Itakura, Phys. Rev. D **92**, 016002 (2015).
- [14] F. Della Valle *et al.*, Phys. Rev. D **90**, 092003 (2014).
- [15] A. Cadene *et al.*, Eur. Phys. J. D **68**, 16 (2014).
- [16] R. Cameron *et al.*, Phys. Rev. D **47**, 3707 (1993).
- [17] K. Homma, D. Habs and T. Tajima, Appl. Phys. B **104**, 769 (2011).
- [18] B. Marx, I. Uschmann, S. Hofer, R. Lotzsch, O. Werhrhan, E. Förster, M. Kaluza, T. Stöhlker, H. Gies, C. Detlefs, T. Roth, J. Härtwig, G.G. Paulus, Opt. Commun. **284**, 915 (2011).
- [19] V. Dinu, T. Heinzl, A. Ilderton, M. Marklund and G. Torgrimsson, Phys. Rev. D **90**, 045025 (2014).
- [20] W. P. Leemans *et al.*, Phys. Rev. Lett. **113**, 245002(2014).
- [21] T. Tajima and J. M. Dawson, Phys. Rev. Lett. **43**, 267(1979).
- [22] C. Joshi *et al.*, Nature **311**, 525 (1984).
- [23] K. D. Shmakov, *Study of nonlinear QED effects in interactions of terawatt laser with high-energy electron beam*, Ph.D thesis, University of Tennessee, 1997, SLAC-R-666, UMI-98-23127, UMI-98-23127-MC.
- [24] C. Bamber *et al.*, Phys. Rev. D **60**, 092004 (1999).
- [25] J. H. Hubbell, H. A. Gimm and I. Øverbø, J. Phys. Chem. Ref. Data **9**, 1023 (1980).
- [26] M. J. Berger *et al.*, XCOM: Photon Cross Section Database (version 1.5), 2010: National Institute of Standards and Technology.
- [27] T. H. Berlin and L. Madansky, Phys. Rev. **78**, 623 (1950).
- [28] C. N. Yang. Phys. Rev. **77**, 722 (1950).
- [29] H. Olsen and L.C. Maximon, Phys. Rev. **114**, 887 (1959).
- [30] L.C. Maximon and H. Olsen, Phys. Rev. **126**, 887 (1962).
- [31] B. Wojtsekhowskia, D. Tedeschib and B. Vlahovicc, Nucl. Instr. Meth. A **515**, 605 (2003).
- [32] C. de Jager *et al.*, Eur. Phys. J. A **19**, 275 (2004).
- [33] D. Bernard, Nucl. Instr. Meth. A **729**, 765-780 (2013).
- [34] S. Agostinelli *et al.*, Nucl. Instr. and Meth. A **506**, 250 (2003).
- [35] J. Allison *et al.*, IEEE Trans. Nucl. Sci. **53**, 270 (2006).